Optical properties of copper and silver in the energy range 2.5–9.0 eV

K. Stahrenberg, Th. Herrmann, K. Wilmers, N. Esser,* and W. Richter
Institut für Festkörperphysik der TU Berlin, Hardenbergstraße 36, 10623 Berlin, Germany

M. J. G. Lee
Department of Physics, University of Toronto, Canada
(Received 23 October 2000; published 31 August 2001)

The optical properties of copper and silver bulk crystals with atomically clean surfaces have been determined experimentally and interpreted in terms of *ab initio* band structure calculations. The dielectric functions are evaluated from spectroscopic ellipsometry data taken in ultrahigh vacuum (UHV) in the spectral range of 2.5–9.0 eV (at room temperature). The data are corrected for surface roughness using results from *ex situ* atomic force microscopy (AFM). Significant differences of detail in the amplitudes and line shape are attributed to the better surface quality of our samples. Density functional calculations of the dielectric functions of copper and silver are carried out, based on models of the valence bands deduced by fitting to experimental Fermi surface and quasiparticle mass data. Small energy shifts, which take into account many-body effects in the final states of the optical transitions in an extended scissors approximation, are needed to bring the calculated dielectric functions into good agreement with the experimental data. The interband transitions associated with individual features in the dielectric function are identified by comparing the energy derivatives of the measured and calculated dielectric functions.

DOI: 10.1103/PhysRevB.64.115111 PACS number(s): 78.20.Ci, 78.40.Kc, 71.15.Ap

I. INTRODUCTION

In a review published in 1986, Palik[1] surveyed more than 30 studies of the dielectric functions of bulk copper and silver, and found only limited data in the visible and vacuum ultraviolet. Since then some new work has been reported on clusters and thin films, but none on the bulk metals. Palik's review reported significant variations among the various published data, presumably due in large part to inadequately characterized samples. Both exposure to air and surface roughness are expected to reduce the measured value of the imaginary part of the dielectric function ε_2, especially in the visible where the reflectivity is high and the skin depth is very small. A common feature of previous studies is that the measurements were made on surfaces that had been exposed to air, and that the roughness of the reflecting surfaces was not determined.

Pells and Shiga [2] measured the optical absorption of copper under vacuum using a polarimetric technique. They found that exposure to oxygen strongly suppresses optical absorption at all photon energies above 2 eV. Their samples were prepared by polishing ingots of polycrystalline copper in air, then vacuum annealing at 5×10^{-9} Torr, but some readsorption of oxygen occurred as the temperature was lowered after annealing. Johnson and Christy [3] prepared surfaces of copper, silver, and gold by evaporation on to fused-quartz substrates at 4×10^{-6} Torr, but their measurements of reflectance and transmission were made in air. In a study by Hagemann *et al.*,[4] copper and silver surfaces were prepared by evaporating thin films on to a collodion substrate, then dissolving away the substrate, so the surfaces were exposed to air before measurement. Leveque *et al.*[5] made *in situ* reflectance measurements on silver films prepared at 5×10^{-7} Torr, but their measurements did not cover the important visible region of the spectrum. In none of these studies was the surface roughness determined.

Many of the previous studies involved Kramers-Kronig analysis of reflectance data, in which assumptions and approximations are unavoidable. An exception is the work of Johnson and Christy,[3] who combined reflectance and transmission measurements at normal incidence with *p*-polarized transmission at 60° to determine the real and imaginary parts of the dielectric function in the visible and the near UV.

The noble metals have been widely used to test theoretical techniques for calculating the electronic properties of *d*-band metals, but relatively little work has been done on their dielectric properties. Janak *et al.*[6] used the KKR method in the spherical approximation to carry out a self-consistent nonrelativistic calculation of the dielectric function of copper. Their calculation involved two parameters that were determined from experimental data. One parameter, the coefficient of Slater's X-α exchange potential, was determined by fitting the ground-state energy bands to the shape of the Fermi surface, and the other, representing the energy dependence of the electron self-energy, was determined by fitting features in the calculated dielectric function to peaks in the ε_2 data of Johnson and Christy.[3] Their fitting procedure greatly improved the agreement with the experimental dielectric function of Pells and Shiga,[2] but there were significant discrepancies with that of Johnson and Christy.[3] Fuster *et al.*[7] carried out a self-consistent full-potential nonrelativistic calculation of the electronic and optical properties of silver, using a local von Barth-Hedin exchange-correlation potential. They noted that the onset of interband transitions is significantly too low in energy in comparison with experiment. This is because their calculation placed the *d* bands too close to the Fermi energy by about 0.7 eV.

Campillo *et al.*[8] reported first-principles pseudopotential calculations of the dynamical density response functions of copper, both in the RPA and in a time-dependent extension of

local density functional theory. Their results reproduce the general features of the experimental ε_2 data, although their calculation appears to overestimate the strength of energy-dependent features. In another recent paper, Cazalilla *et al.*[9] reported a similar calculation for silver. While their paper focussed on the energy-loss spectrum, they also compared the dielectric function with the data of Winsemius *et al.*[10] as reported by Lynch and Hunter.[13] They too noted that the onset of interband transitions is significantly too low in energy in comparison with experiment, and they suggested that this may be because the LDA does not adequately take into account correlations within the narrow *d*-like energy bands of silver.

The GW approximation (GWA) to the electron self-energy is widely used to treat correlation effects in optically-excited electron systems.[11,12] However, to the best of our knowledge no such calculations have yet been reported for the dielectric function of noble metals. Provided that the energy shifts for excitation energies calculated in the GWA are only weakly dependent on the band index and the *k* point, they can be approximated by a rigid shift, a method known as scissors operator approach.[14] The actual amount of that shift for electronic states close to the Fermi energy can be determined from a comparison between the calculated and the measured dielectric function in the visible and vacuum ultraviolet.

The present study is the first to exploit current techniques of surface preparation and surface characterization. It was carried out using a UHV ellipsometer mounted in a synchrotron beam line. Contamination-free (110) surfaces of single crystal samples of Cu and Ag were prepared *in situ* by ion sputtering and annealing. The surface preparation was checked by observing transitions between surface electronic states by reflection anisotropy spectroscopy (RAS). Transitions between localized surface states at the $\bar{Y}$ point of the surface Brillouin zone give rise to features in RAS data at 2.1 eV on clean Cu(110) and at 1.7 eV on clean Ag (110).[16,18] Very small amounts of contaminants suffice to quench these features, so their appearance in RAS data is a sensitive test of a clean adsorbate-free surface. Ellipsometry was used to measure independently the real and imaginary parts of the dielectric function, thereby avoiding the approximations involved in Kramers-Kronig analysis of experimental data. To take into account the surface roughness that results from ion sputtering and annealing, the roughness of the reflecting surfaces was measured *ex situ* by means of atomic force microscopy, and the dielectric functions were corrected using an effective medium model.

In the present study, self-consistent relativistic full-potential calculations of the dielectric functions of copper and silver were carried out on the basis of density functional theory, and the results were compared with the experimental data. The sensitivity to energy-dependent features of the dielectric functions was greatly enhanced by comparing also their energy derivatives. *Ab initio* calculations, in which the exchange-correlation potentials were evaluated in the generalized gradient approximation (GGA), yielded results that are not in satisfactory agreement with experiment. This is in part because, as in previous work based on DFT, the calculated threshold for interband transitions is too low in energy. We obtained much better agreement with experiment when, following the approach of Janak *et al.*,[6] we modeled the ground state energy bands by using an empirical exchange-correlation potential that was adjusted to fit experimental Fermi surface and quasiparticle mass data. We conclude that the principal reason why our empirical dielectric function calculations are in better agreement with experiment is that they generate a more accurate configuration of the ground-state energy bands that are the initial states of the optical transitions.

Scissors shifts were extracted by fitting the remaining discrepancies between the experimental and the calculated dielectric functions. The scissors shifts prove to be small and of similar magnitude for copper and silver, showing that effects beyond DFT play at most a minor role in determining the dielectric functions of the noble metals in the visible and the vacuum ultraviolet.

The present paper is organized as follows. Experimental details of the RAS, ellipsometry, and surface roughness measurements are reported in Sec. II. In Sec. III the theory underlying the dielectric function calculations is outlined, and the values adopted for the parameters are reported. Our results for copper are presented and discussed in Sec. IV A, and for silver in Sec. IV B. Finally, Sec. V summarizes the results and conclusions of the present work.

II. EXPERIMENTAL

The experiments were performed in an ultrahigh vacuum chamber at the 2m-Seya-Namioka beamline at BESSY I synchrotron in Berlin. We used single crystal Cu(110) and Ag(110) samples. The crystals were aligned with Laue x-ray backscattering to within 0.1° and mechanically polished before being introduced into the chamber. *In situ* cleaning of the surfaces was done using cycles of sputtering with 600 eV argon ions at room temperature and subsequent annealing to 670 K.

The surface preparation was checked by means of reflectance anisotropy spectroscopy (RAS) after each cycle of sputtering and annealing. The spectrometer, which was attached to the chamber through a low strain quartz window, covers the spectral range from 1.5 to 5.5 eV. Details of the spectrometer can be found elsewhere.[15,16] RAS measures the difference between the complex reflectivities for polarization along two perpendicular axes (in our case $[1\bar{1}0]$ and [001]) within the surface. For (110) surfaces of fcc metals it has been shown that electronic transitions between surface states are responsible for characteristic RAS features at 2.1 eV on Cu(110) and 1.7 eV on Ag(110).[16–18] Thus, RAS can be used in a similar way to valence-band photoemission spectroscopy to check the surface conditions. After the surface state transitions appeared in the reflectance anisotropy spectrum, the surfaces were judged to be clean.

The ellipsometry measurements were performed using a rotating analyzer ellipsometer operating with synchrotron radiation in the spectral range from the visible to the vacuum-UV. All of the optical components (polarizers, analyzer, sample, and Si photodiode) were mounted inside the vacuum

chamber. In the ellipsometry measurements, the plane of incidence was defined by the surface normal and the $[1\bar{1}1]$ direction in the sample surface. A detailed description of the ellipsometer is given elsewhere.[19] In brief, the light from the 2m-Seya monochromator passes through an MgF_2 prism before illuminating the sample, and the reflected light is analyzed by a second rotating MgF_2 prism. The angle of incidence is fixed at 67.5°. This configuration works between 2.5 and 10 eV. Between 2.5 and 4.5 eV an additional quartz filter in the reflected beam is used to suppress second order light from the monochromator. This configuration gives superior accuracy compared to any laboratory ellipsometer since the sample and all optical components are under well-defined UHV conditions. Also, artifacts such as those induced by the windows of a UHV chamber are completely absent.

Ion sputtering and annealing removes surface contamination, but the resulting surface may not be ideally flat. Since the surface roughness modifies the optical response, the samples were measured in air with an atomic force microscope (AFM) after the completion of the ellipsometry experiments. The AFM measurements were carried out in contact mode using a Digital Instruments Nanoscope III. The RMS roughness was calculated from the height profile of the scanned areas (500×500 nm). As described in Sec. IV the dielectric functions of Cu and Ag bulk were estimated in a three-layer model using the ellipsometry and AFM data.

III. THEORY

In the limit of low momentum transfer, the dielectric function of a metal can be expressed as[20,21]

$$\varepsilon(\omega)=1-\frac{(e^2/3\pi^2\hbar)\int v_F dS_F}{\omega^2+i\omega/\tau}+\varepsilon^i(\omega). \tag{1}$$

The first two (Drude) terms represent the contribution of intraband transitions, while $\varepsilon^i(\omega)$ represents the contribution of interband transitions. In an intraband transition, excess momentum is transferred to the lattice by phonon or impurity scattering. Assuming that the relaxation time τ is isotropic, Eq. (1) can be used to calculate the intraband contribution to the dielectric function from the electronic energy bands in the vicinity of the Fermi level.

As the wave vector of a photon is typically much smaller than the size of the Brillouin zone, it is an excellent approximation to treat interband optical transitions as k conserving. In this approximation, the imaginary part of the interband contribution to the dielectric function at frequency ω and temperature 0 K can be evaluated from the expression[14,22]

$$\varepsilon_2^i(\omega)=\frac{4\hbar^2e^2}{\pi\omega^2}\sum_{m,n}\int_{S_F}dS_F\frac{|\int d^3r\Psi^*_{n,k}\vec{\epsilon}\cdot\vec{v}\Psi_{m,k}|^2}{|\nabla_k(E_n-E_m)|_{E_n-E_m=\hbar\omega}}, \tag{2}$$

where m and n denote the occupied initial and unoccupied final states of wave vector k, E_m, and E_n are the corresponding energies, $\vec{\epsilon}$ is the polarization vector of the incident light, and the matrix element of the velocity $\vec{v}$ is evaluated between the eigenvectors that correspond to the initial and final states of the optical transition. From the imaginary part of the interband contribution to the dielectric function, the real part can be readily calculated by Kramers-Kronig inversion.[22]

Studies of many systems have shown that density functional calculations within the local density approximation (LDA) and the generalized gradient approximation tend to underestimate the energies of excitation.[23] One approach to try to address the limitations of density functional theory (DFT) for excitations from the ground state is the GW formalism.[24,25] If the k-dependence of the error in the excitation energies is negligible, i.e., if

$$\Delta(k)=[E_n(k)-E_m(k)]_{\mathrm{GW}}-[E_n(k)-E_m(k)]_{\mathrm{DFT}}\approx\Delta, \tag{3}$$

$\varepsilon_2^{\mathrm{GW}}(\hbar\omega)$ can be obtained by shifting $\varepsilon_2^{\mathrm{DFT}}(\hbar\omega)$ along the energy axis,

$$\varepsilon_2^{\mathrm{GW}}(\hbar\omega)=\varepsilon_2^{\mathrm{DFT}}(\hbar\omega-\Delta). \tag{4}$$

This result,[14] which takes into account the nonlocality of the self-energy and is consistent with the requirement of gauge invariance, is the formal basis for the *scissors approximation* that is widely used to correct the results of density functional calculations of the dielectric function.

The electronic structures of copper and silver have been calculated semirelativistically by means of the full-potential linear augmented plane wave (FP-LAPW) method using the WIEN97 code.[26] The electronic energies were determined self-consistently by solving the Kohn-Sham equations of density-functional theory. The spin-orbit interaction term was included in the Hamiltonian. Exchange and correlation with the average electron distribution were represented by a one-electron potential derived by Perdew *et al.*[27] in the generalized gradient approximation, an extension of the LDA that includes additional terms that involve the gradient of the electron density. This potential is regarded as being among the most accurate of the current generation of *ab initio* exchange-correlation potentials.

The following are the parameters adopted for the calculations. For copper at room temperature, the edge of the conventional cubic unit cell is 6.8087 a.u. and the sphere radius was set to 2.20 a.u. For silver at room temperature, the edge of the conventional cubic unit cell is 7.7218 au and the sphere radius was set to 2.73 a.u. Within the sphere, the charge density and potential were expanded in cubic harmonics up to $L=9$, and a plane wave expansion involving 9261 Fourier coefficients was used in the interstitial region. The Brillouin zone integrals for the Fermi energies were evaluated numerically on a grid of 286 reduced k points, while the dielectric functions were derived from joint densities of states and matrix elements evaluated on a grid of 11 480 reduced k points. Checks showed that these grids are sufficiently fine to ensure satisfactory convergence.

IV. RESULTS AND DISCUSSION

The spectroscopic ellipsometry data yield a pseudodielectric function that depends, in an inhomogeneous system like a multilayer sample, on the dielectric properties of each layer

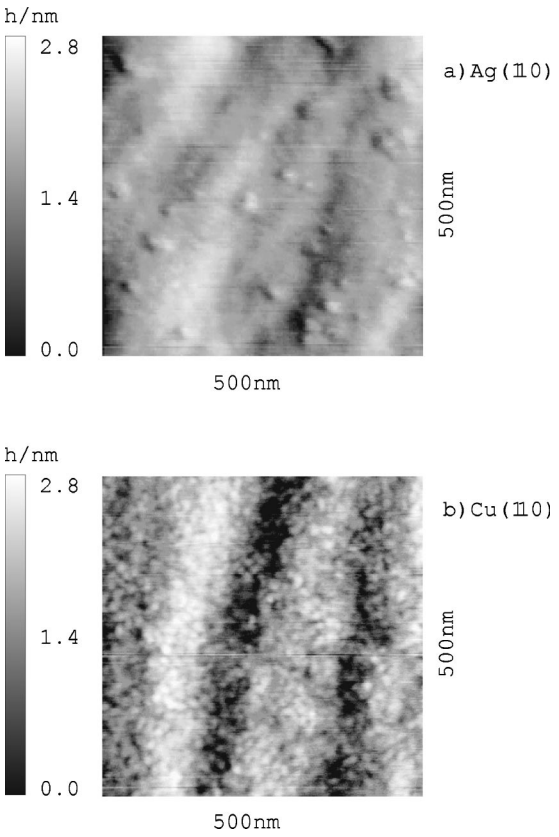

FIG. 1. AFM images of the copper and silver samples. The images were taken in air after the completion of the optical experiments. The AFM microscope was used in contact mode. From the height profile the root mean square (RMS) roughness was calculated. a) Ag(110), RMS roughness 0.42 nm, b) Cu(110), RMS roughness 0.41 nm.

within the penetration depth of the light. For bulk crystals as investigated here, the sample consists of the semi-infinite bulk metal plus a thin, usually ill-defined, surface layer of distinct dielectric properties, which represents adsorbed overlayers (contamination) and surface roughness. In order to extract the bulk dielectric function, the properties of the surface layer must be known and corrected for by means of an appropriate model. This is possible only if the thickness and optical properties of the overlayers are known, a requirement that is generally not fulfilled. Therefore we present in the following ellipsometry data that were collected under UHV conditions on atomically clean, well ordered Cu(110) and Ag(110) surfaces. Even at a clean surface there is a thin surface layer with dielectric properties different from the bulk, but this effect is very small compared with a contaminated surface under non-UHV conditions.

The clean surfaces of Cu(110) and Ag(110) are not ideally flat on an atomic scale, and it is known that surface roughness lowers the value of $\langle \varepsilon_2 \rangle$ in the spectral region of interband transitions.[5,28] In Fig. 1, AFM images are shown that were taken in air after the completion of the optical experiments. r.m.s. surface roughnesses of 0.41 and 0.42 nm were found for Cu and Ag, respectively. These RMS values were used to correct the measured dielectric function for surface roughness. A three-layer model consisting of the bulk, the rough surface layer and the vacuum was used to extract the bulk dielectric function. An effective medium model due to Bruggeman was used to describe the thin surface layer (thickness $d \ll \lambda$) as a mix of 50% voids in 50% bulk matrix.[29]

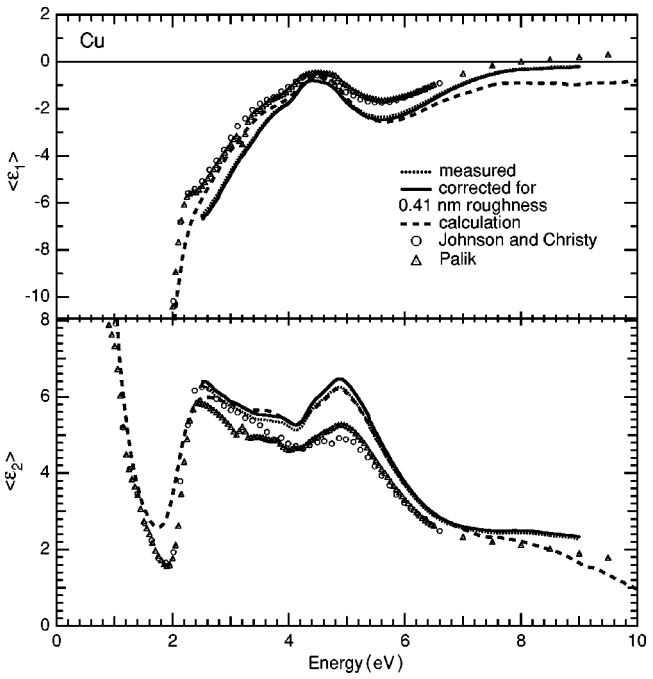

FIG. 2. Real part (upper graph) and imaginary part (lower graph) of the dielelectric function of Cu. The dotted line shows the measured dielectric function and the solid line shows the dielectric function after correcting for surface roughness. The dashed line shows the results of the present calculation. Included are data from the literature: squares from Ref. 1 and dots from Ref. 3.

A. Copper

The ellipsometry data for Cu are shown in Fig. 2. The dielectric function as measured on clean Cu(110) is shown (dotted line), together with the bulk dielectric function after correcting for surface roughness (solid line), and the dielectric function obtained from the FP-LAPW calculation (dashed line). Representative data from the literature are plotted for comparison.

The surface roughness correction is rather small, the maximum increase in $\langle \varepsilon_2 \rangle$ amounting to 0.2 at 4.5 eV. However, our values of $\langle \varepsilon_2 \rangle$ are considerably higher (by 1.0 to 1.5 at 4.5 eV) than the dielectric functions determined from reflectance measurements in Refs. 1 and 3. We attribute this difference to the better surface quality of our samples, and in particular to the absence of adsorbed overlayers. Our data also show clearly a shoulder in $\langle \varepsilon_2 \rangle$ around 4.4 eV that was hardly resolved in previous data.

The electronic energy bands of copper calculated self-consistently by means of density functional theory in the GGA are plotted as solid lines in Fig. 3. The bands are numbered starting from the lowest band at a given k. Below the Fermi level, a broad s-p band is crossed by, and hybridizes with, a relatively narrow set of five d bands, the topmost of

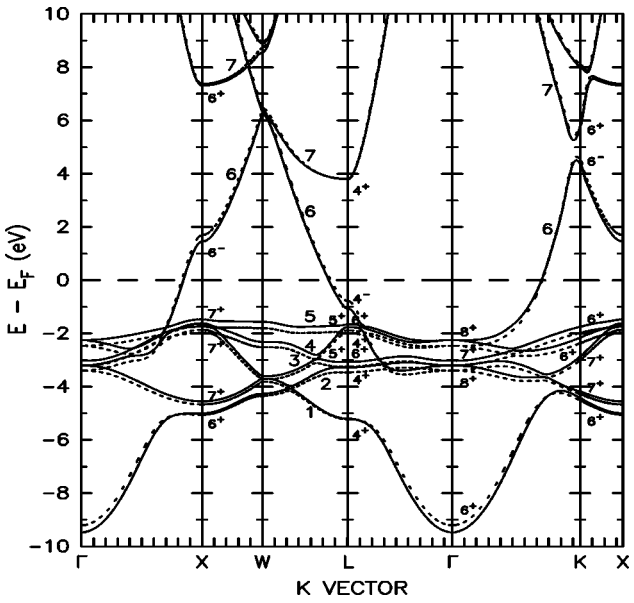

FIG. 3. Calculated band structure of copper. The solid lines show the energy bands as determined from our *ab initio* density functional calculation in which exchange and correlation were treated in the GGA. The dotted lines show the bands calculated using the empirical exchange-correlation potential described in the text. The labels n^+, n^- denote the symmetries of the relativistic electron states at special points of the Brillouin zone. The bands are numbered, as in the text, starting from the lowest band at a given *k*.

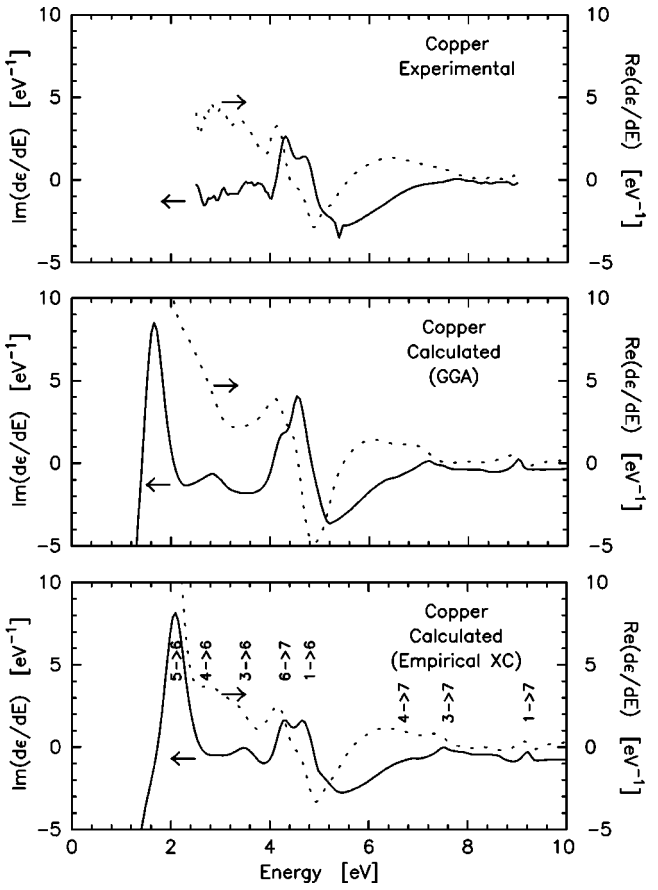

FIG. 4. Comparison between the energy derivative of our experimental dielectric function for copper (upper graph), the result of our *ab initio* density functional calculation in the GGA (middle), and our result based on the empirical exchange-correlation potential (lower graph). In the lower graph the interband transitions that account for the principal features in the dielectric function are identified according to the calculation. The calculated dielectric functions include small final-state dependent scissors shifts as described in the text.

which lies about 1.5 eV below the Fermi level. These energy bands and the corresponding eigenvectors were used to calculate the dielectric function of copper in the limit of low momentum transfer.

The derivative of the experimental dielectric function with respect to the photon energy was calculated numerically in order to enhance the energy-dependent features of the spectrum. The real and imaginary parts of the experimental $d\varepsilon(\omega)/dE$ are plotted in the upper panel of Fig. 4. In order to interpret the various features in the data, the band-resolved derivative spectrum of $\varepsilon_2(\omega)$ was also calculated, from which the contributions of transitions between all possible pairs of initial and final state bands could be identified.

The most prominent features of the experimental $d\varepsilon_2(\omega)/dE$ are two maxima at 4.3 and 4.7 eV that correspond to the shoulder and the maximum in $\varepsilon_2(\omega)$ discussed above. In the calculated $d\varepsilon_2(\omega)/dE$ there are two prominent peaks in the same energy range. The peak at 4.0 eV is due to transitions from band 6 to band 7, while the peak at 4.7 eV is due to transitions from band 1 to band 6. No single scissors shift Δ can bring the energies of these two calculated peaks fully into agreement with experiment. The fact that final states in band 6 are predominantly *p*-like, while final states in band 7 are predominantly *s*-like, suggested a simple *ansatz*, in the spirit of the scissors approximation, in which the energy shift Δ depends on the final state band. The only set of non-negative scissors shifts that brings the energies of these two peaks into agreement with experiment is $\Delta_6 = 0.0$ eV and $\Delta_7 = 0.3$ eV.

The calculated $d\varepsilon_2(\omega)/dE$, including the scissors shifts, is plotted in the center panel of Fig. 4. The strong peak at 1.65 eV, due to transitions from occupied states in band 5 to unoccupied states in band 6, marks the onset of interband transitions. This peak is below the range of the present experimental data, but it has been observed by others at about 2.10 eV.[3,1] There is also a weak peak at 2.8 eV due to transitions from band 3 to band 6, a broad hump at about 6.3 eV due to transitions from band 4 to band 7, and a weak peak at 7.2 eV due to transitions from band 3 to band 7. For each of these, a corresponding feature appears in the experimental data at a significantly higher energy.

These discrepancies between the calculated $d\varepsilon_2(\omega)/dE$ and the experimental data all suggest that the present density functional calculation places the *d*-band complex too high relative to the *s*-*p* band and the Fermi energy. Similar discrepancies have been noted between density-functional calculations and experimental data for such ground state properties of copper as the shape of the Fermi surface and the many-body enhancement of the quasiparticle velocity, both

of which are strongly influenced by hybridization between the valence *s*-*p* band and the *d*-band complex.[30–33] Significant discrepancies are found irrespective of whether the exchange and correlation are treated in the LDA or GGA.[31] This is surprising, because density functional theory is expected to work well for such ground state properties as the energies of the valence bands.

The exchange-correlation potential is perhaps the greatest source of uncertainty in calculating ground state properties on the basis of DFT. The present results suggest that, for copper, even the best of the current generation of *ab initio* exchange-correlation potentials yield *d* bands that are too high relative to the *s*-*p* band. Increasing the strength of the exchange potential lowers the *d* bands and raises the *s*-*p* bands relative to the Fermi level. By adjusting the coefficient of the exchange term it is possible to generate ground-state energy bands for copper that are in good agreement with experimental Fermi surface and quasiparticle mass data.[6,32,33,30] The energy bands calculated from an empirical exchange-correlation potential for copper constructed in this way are plotted as dotted lines in Fig. 3. Compared with the *ab initio* calculation, the top of the *d*-band is lowered by as much as 0.3 eV relative to the Fermi level.

The dielectric function $\varepsilon(\omega)$ was also calculated from the empirical exchange-correlation potential. Small scissors shifts of the final state bands ($\Delta_6=0.2$ eV and $\Delta_7=0.4$ eV) were needed to bring the energies of the most prominent peaks into agreement with experiment. The real and imaginary parts of the calculated $d\varepsilon(\omega)/dE$ are plotted in the lower panel of Fig. 4, and in Fig. 2 the real and imaginary parts of $\varepsilon(\omega)$ are compared with the experimental dielectric function. The calculated dielectric function is in very good overall agreement with the experimental data. Work is continuing to refine the empirical exchange-correlation potential. However, since the dielectric function is much less sensitive to the valence band configuration than is the Fermi surface, further refinements are not expected to bring about a significant change in the calculated dielectric function. Details of the empirical exchange-correlation potential will be reported elsewhere.[30]

Scattering by phonons and defects results in lifetime broadening of the optical transitions that contribute to $\varepsilon(\omega)$. The best agreement with the strengths of the various features observed in the present experimental data for copper at room temperature was found with an assumed energy broadening $\gamma=0.15\,\text{eV}\approx 6\ kT$. That γ is much larger than kT suggests that, in the copper samples used in the present work, phonon scattering is dominated by other scattering processes. Close to the minimum in $\varepsilon_2(\omega)$ at a photon energy of 2.0 eV (Fig. 2), there is a significant discrepancy between the results of the present calculation and experimental data taken from literature.[3,1] This discrepancy is largely removed if the dielectric function is recalculated assuming much weaker scattering ($\gamma=0.025$ eV$\approx kT$).

B. Silver

In Fig. 5 the measured dielectric function $\langle\varepsilon\rangle$ of silver in the energy range 2.5–9.7 eV is shown (dotted line), together with the bulk dielectric function after correction for surface roughness (solid line), and the result of our FP-LAPW calculation (dashed line). Representative data from the literature are also shown. Below the onset of *d*-band absorption at 3.84 eV,[5] the noise in our $\langle\varepsilon_2\rangle$ data increases since the sample is nonabsorbing and no compensator could be used in the experimental setup.

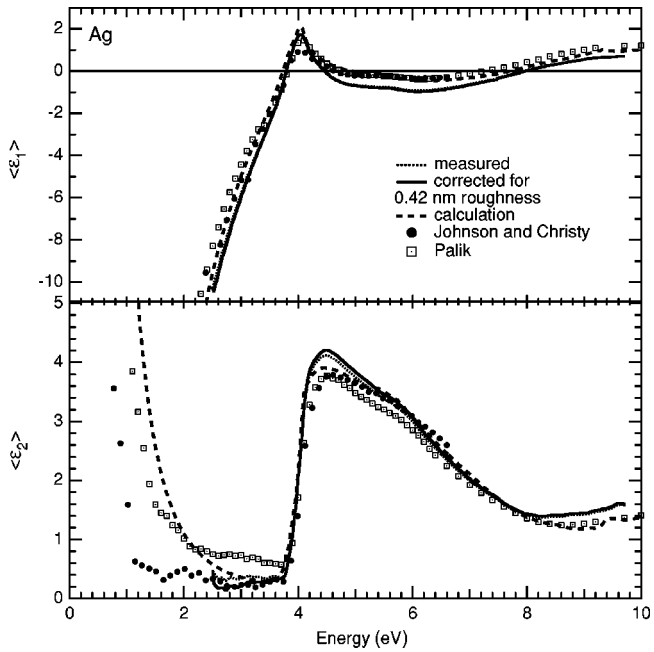

FIG. 5. Real part (upper graph) and imaginary part (lower graph) of the dielelectric function of Ag. The dotted line shows the measured dielectric function and the solid line shows the dielectric function after correcting for surface roughness. The dashed line shows the results of the present calculation. Included are data from the literature: squares from Ref. 1 and dots from Ref. 3.

As for Cu, the correction for surface roughness turns out to be small (see Fig. 1), increasing $\langle\varepsilon_2\rangle$ by only 0.1 at 4.5 eV. However, our ε_2 is significantly higher (by 0.5 at 4.5 eV) than in representative data from the literature,[3,1] and $\langle\varepsilon_1\rangle$ is also significantly different. As a consequence, the energies where ε_1 is equal to zero differ from those in the earlier data. In particular, the zero crossing observed at 7.3 eV in Ref. 1 is shifted to 7.95 eV in our data. While our dielectric function is in overall agreement with the literature, the features are sharpened. The data in the literature were derived from reflectance measurements on thin films and polycrystalline samples that were not cleaned and measured under UHV conditions, so the discrepancies are most likely due to the presence of adsorbate overlayers in the earlier experiments.

Plasmon excitations are expected to occur at those energies where $\varepsilon_1=0$ and the first derivative of ε_1 is positive.[34] In silver, ε_1 crosses from negative to positive at 3.79 eV and again at 7.95 eV (see Fig. 5), and energy loss peaks have been observed at both energies.[35] The feature at 7.95 eV has been interpreted as a remainder of the free electron excitation.[34] Another interpretation involves the splitting of the theoretical plasma frequency into two hybrid plasmons.[36] For the lower energy plasmon the *s* electrons are screened by

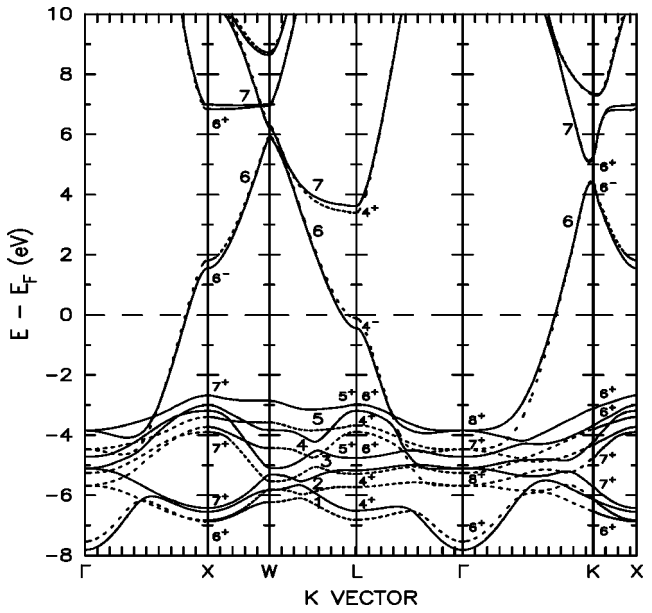

FIG. 6. Calculated band structure of silver. The solid lines show the energy bands as determined from our *ab initio* density functional calculation in which exchange and correlation were treated in the GGA. The dotted lines show the bands calculated using the empirical exchange-correlation potential described in the text. The labels n^+, n^- denote the symmetries of the relativistic electron states at special points of the Brillouin zone. The bands are numbered, as in the text, starting from the lowest band at a given k.

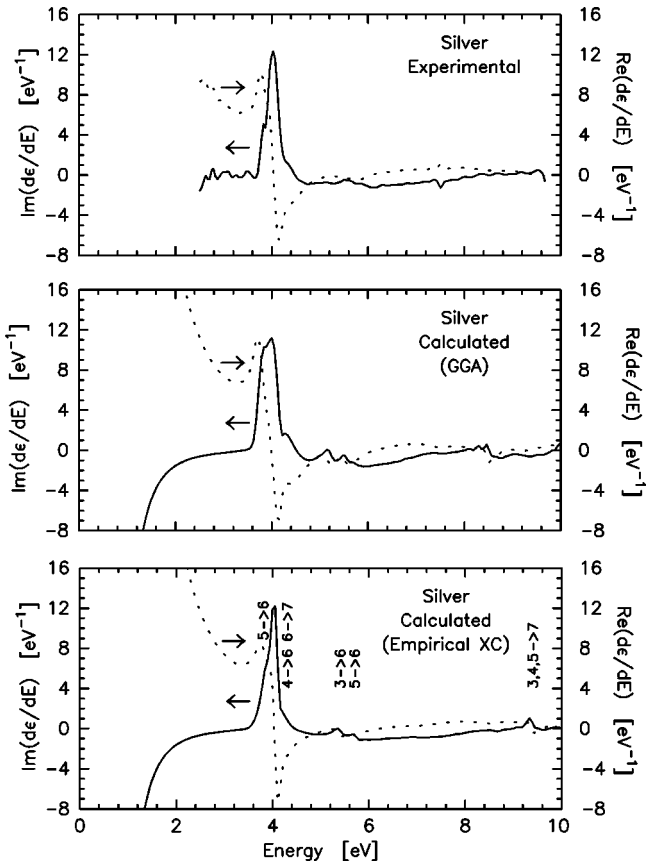

FIG. 7. Comparison between the energy derivative of our experimental dielectric function for silver (upper graph), the result of our *ab initio* density functional calculation in the GGA (middle), and our result based on the empirical exchange-correlation potential (lower graph). In the lower graph the interband transitions that account for the principal features in the dielectric function are identified according to the calculation. The calculated dielectric functions include small final-state dependent scissors shifts as described in the text.

the *d* electrons, while for the higher energy plasmon one may think of the *d* and *s* electrons with their polarizations being in phase.[36]

The electronic energy bands of silver based on *ab initio* self-consistent relativistic FP-LAPW calculations in which the spin-orbit interaction was included and exchange and correlation were treated in the GGA, are plotted as solid lines in Fig. 6. As for copper, a broad *s*-*p* band is crossed by, and hybridizes with, a relatively narrow set of five *d* bands. According to the calculation, the highest *d* band lies about 2.7 eV below the Fermi level. The dielectric function of silver in the limit of low momentum transfer has been calculated from these energy bands and the corresponding eigenvectors.

The energy derivative of the experimental dielectric function of silver is plotted in the upper panel of Fig. 7. The most prominent features of the experimental $d\varepsilon_2(\omega)/dE$ are a strong peak at 4.03 eV and a weaker overlapping shoulder at 3.84 eV. The data also show a shoulder at 4.2 eV. The most prominent features of the calculated $d\varepsilon_2(\omega)/dE$ are a strong peak due to transitions from band 5 to band 6 at 3.10 eV and a weaker peak due to transitions from band 6 to band 7 at 3.75 eV. As in copper, no simple scissors shift Δ can bring the calculated dielectric function into agreement with experiment, so the scissors shift was allowed us to depend on the final state band. Of the two sets of non-negative scissors shifts that can bring the most prominent peaks of the calculated dielectric function into agreement with experiment, only $\Delta_6=0.93$ eV and $\Delta_7=0.09$ eV is consistent with the shoulder observed experimentally at 4.2 eV, where the alternative set of scissors shifts predicts a dip. The resulting $d\varepsilon_2(\omega)/dE$ is plotted in the center panel of Fig. 7. The calculated shoulder at 3.84 eV is comparable in strength to the peak at 4.03 eV, while in the experimental data the shoulder is much weaker than the peak.

Density functional calculations of such ground state properties of silver as the shape of the Fermi surface and the many-body enhancement of the quasiparticle mass give results that are in significant disagreement with the experimental data.[32,33] This suggests that one reason why our *ab initio* calculation yields a dielectric function that is not fully in agreement with experiment is that, as for copper, it produces an inaccurate configuration of initial states. To explore this possibility, a calculation of the dielectric function of silver was carried out based on an empirical exchange-correlation potential that was constructed by fitting experimental Fermi surface and quasiparticle mass data.[30] Small final-state energy shifts $\Delta_6=0.18$ eV and $\Delta_7=0.60$ eV were needed to bring the most prominent peaks of the calculated dielectric function into agreement with the experimental data. The resulting dielectric function is plotted in the lower panel of Fig. 7.

The agreement with experiment is significantly better than for our *ab initio* calculation in which exchange and correlation were treated in the GGA. In particular, the strength of the shoulder at 3.84 eV is about one half of that of the peak at 4.03 eV, as is found experimentally. Moreover, the final state energy shifts are both weaker and less dependent on the final state band. The main reason why the empirical exchange-correlation potential yields a more accurate dielectric function for silver is that it generates a more accurate model of the ground-state energy bands.

The best agreement with the various features observed in the present experimental data for silver at room temperature was found with an assumed energy broadening $\gamma = 0.025$ eV$\approx kT$. That γ is comparable to kT suggests that, in the silver samples used in the present experiments, scattering of the conduction electrons is dominated by thermal phonons.

V. SUMMARY

In situ ellipsometry measurements on atomically clean Cu and Ag samples prepared in UHV are presented and compared with calculated dielectric functions based upon DFT. For both metals, the absolute values and the overall form of the dielectric function show significant differences as compared with data from the literature that are based on reflectance measurements under non-UHV conditions. We attribute these differences to the better quality of the surfaces of our samples, mainly due to the absence of adsorbed overlayers.

Our numerical results show that *ab initio* calculations based on DFT and using the best of the current generation of exchange-correlation potentials yield dielectric functions for copper and silver that are significantly in disagreement with the experimental data. This is partly because DFT is not strictly applicable to calculating the properties of excitations, but a large part of the discrepancy is traced to an inaccurate configuration of the ground-state energy bands that are the initial states of the optical transitions. Density functional calculations based on empirical exchange-correlation potentials that were derived by fitting experimental Fermi surface and quasiparticle mass data yield dielectric functions that are in much better agreement with the experimental data. The residual discrepancies are fitted by final-state-dependent scissors shifts that prove to be small and of similar magnitude for copper and silver, showing that effects beyond DFT play at most a minor role in determining their dielectric functions.

ACKNOWLEDGMENTS

We thank C. Ambrosch-Draxl, P. Blaha, J.M. Perz, A. Shkrebtii, Adolfo Eguiluz, Wolf-Gero Schmidt, and J.E. Sipe for helpful discussions and comments. Also we would like to thank the staff at BESSY for technical support during the synchrotron experiments and K. Fleischer for the help with the AFM. This work was supported by the Deutsche Forschungsgemeinschaft (DFG) under Grant Nos. Ri/208 32-1 and SFB 290 and by the Bundesministerium für Bildung und Forschung (BMBF) under Grant No. 05 622 ESA2. This work was supported in part by an operating grant from the Natural Sciences and Engineering Research Council of Canada.

*Corresponding author. E-mail address: Norbert.Esser@tu-berlin.de

[1] *Handbook of Optical Constants of Solids,* edited by E. D. Palik (Academic Press, New York, 1985), p. 275.
[2] G. P. Pells and M. Shiga, J. Phys. C **2**, 1835 (1969).
[3] P. B. Johnson and R. W. Christy, Phys. Rev. B **6**, 4370 (1972).
[4] H. J. Hagemann, W. Gudat, and C. Kunz, J. Opt. Soc. Am. **65**, 742 (1975) (Cu 13.8 to 1237 nm).
[5] G. Leveque, C. G. Olson, and D. W. Lynch, Phys. Rev. B **27**, 4654 (1983).
[6] J. F. Janak, A. R. Williams, and V. I. Moruzzi, Phys. Rev. B **11**, 1522 (1975).
[7] G. Fuster, J. M. Tyler, N. E. Brener, J. Callaway, and D. Bagayoko, Phys. Rev. B **42**, 7322 (1990).
[8] I. Campillo, A. Rubio, and J. M. Pitarke, Phys. Rev. B **59**, 12 188 (1999).
[9] M. A. Cazalilla, J. S. Dolado, A. Rubio, and P. M. Echenique, Phys. Rev. B **61**, 8033 (2000).
[10] P. Winsemius, F. F. van Kampen, H. P. Lengkeek, and C. G. van Went, J. Phys. F: Met. Phys. **6**, 1583 (1976).
[11] L.X. Benedict and E.L. Shirley, Phys. Rev. B **59**, 5441 (1999).
[12] S. Albrecht, L. Reining, R. Del Sole, and G. Onida, Phys. Rev. Lett. **80**, 4510 (1998).
[13] D. W. Lynch and W. R. Hunter, in *Handbook of Optical Constants of Solids*, edited by E. D. Palik (Academic Press, New York, 1985), p. 275.
[14] R. DelSole and R. Girlanda, Phys. Rev. B **48**, 11 789 (1993).
[15] W. Richter and J.-T. Zettler, Appl. Surf. Sci. **100/101**, 465 (1996).
[16] K. Stahrenberg, T. Herrmann, N. Esser, J. Sahm, W. Richter, S. V. Hoffmann, and Ph. Hofmann, Phys. Rev. B **58**, R10 207 (1998).
[17] Ph. Hofmann, K. C. Rose, V. Fernandez, A. M. Bradshaw, and W. Richter, Phys. Rev. Lett. **75**, 2039 (1995).
[18] K. Stahrenberg, Th. Herrmann, N. Esser, and W. Richter, Phys. Rev. B **61**, 3043 (2000).
[19] T. Wethkamp, K. Wilmers, N. Esser, W. Richter, O. Ambacher, H. Angerer, G. Jungk, R. L. Johnson, and M. Cardona, Thin Solid Films **313-314**, 745 (1998).
[20] See, e.g., D. Pines, *Elementary Excitations in Solids* (Benjamin, New York, 1964).
[21] See, e.g., J. M. Ziman, *Principles of the Theory of Solids* (Cambridge University Press, London, 1964).
[22] See, e.g., F. Bassani and G. Pastori Parravicini, in *Electronic States and Optical Transitions in Solids*, edited by R. A. Ballinger (Pergamon, London, 1975).
[23] W. E. Pickett, Comments Solid State Phys. **12**, 57 (1986).
[24] M. S. Hybertsen and S. G. Louie, Phys. Rev. B **34**, 5390 (1986).
[25] Z. H. Levine and D. C. Allan, Phys. Rev. B **43**, 4187 (1991).
[26] P. Blaha, K. Schwarz, and J. Luitz, WIEN97, Vienna University of Technology, 1997. (Improved and updated UNIX version of the original copyrighted WIEN code [P. Blaha, K. Schwarz, P. Sorantin, and S. B. Trickey, Comput. Phys. Commun. **59**, 399 (1990)].)

[27] J. P. Perdew, J. A. Chevary, S. H. Vosko, K. A. Jackson, M. R. Pederson, D. J. Singh, and C. Fiolhais, Phys. Rev. B **46**, 6671 (1992).
[28] D. E. Aspnes, J. B. Theeten, and F. Hottier, Phys. Rev. B **20**, 3292 (1997).
[29] *Optical Characterization of Epitaxial Semiconductor Layers*, edited by G. Bauer and W. Richter (Springer, Berlin, 1996).
[30] J. M. Perz and M. J. G. Lee (unpublished).
[31] R. Ahuja, S. Auluck, P. Söderlind, O. Eriksson, J. M. Wills, and B. Johansson, Phys. Rev. B **50**, 11 183 (1994).
[32] H. Eckardt, L. Fritsche, and J. Noffke, J. Phys. F: Met. Phys. **14**, 97 (1984).
[33] R. Ahuja, A. K. Solanki, T. Nautijal, and S. Auluck, Pramana, J. Phys. **32**, 831 (1989).
[34] M. Rocca, Surf. Sci. Rep. **22**, 11 (1995).
[35] T. Bornemann, J. Eickmans, and A. Otto, Solid State Commun. **65**, 381 (1988).
[36] A. Otto and E. Petri, Solid State Commun. **20**, 823 (1976).